Systems & Control Transactions

Research Article - Peer Reviewed Conference Proceeding
ESCAPE 35 - European Symposium on Computer Aided Process Engineering
Ghent, Belgium. 6-9 July 2025
Jan F.M. Van Impe, Grégoire Léonard, Satyajeet S. Bhonsale, Monika E. Polańska, Filip Logist (Eds.)

PSE PRESS

Modular and Heterogeneous Electrolysis Systems: a System Flexibility Comparison

Hannes Lange[a,b*], Michael Große[b,c], Isabell Viedt[a,b], Leon Urbas[b,c]

[a]TUD Dresden University of Technology, Process-to-Order Group, Process Systems Engineering Group
[b]TUD Dresden University of Technology, Process-to-Order Group, P2O Lab Learning Factory
[c]TUD Dresden University of Technology, Process-to-Order Group, Chair of Process Control Systems
*Corresponding author: hannes.lange1@tu-dresden.de

ABSTRACT

Green hydrogen will play a key role in the decarbonization of the steel sector via the direct reduction path [1]. To meet the demand side, both a highly efficient numbering-up based scaling strategy for water electrolysis is needed as well as flexible operation strategies that follow the fluctuating electricity load. This paper presents a modularization approach for electrolysis systems that addresses both aspects by combining different electrolysis technologies into one heterogeneous electrolysis system. We present a modular design of such a heterogeneous electrolysis system that can be scaled for large-scale applications. The impact of different degrees of technological and production capacity-related heterogeneity is investigated using system co-simulation to find an optimal solution for the goal-conflict, that the direct reduction of iron for green steel production requires a constant stream of hydrogen while the renewable electricity profile is fluctuating. For this use-case the distribution of technology and production capacity in the heterogeneous plant layout is optimized regarding overall system efficiency and the ability to follow flexible electricity profiles. The simulation results are compared with conventional homogenous electrolyser plant layouts. First results underline the benefits of combining different technologies and production capacities of individual systems in a large-scale heterogeneous electrolyser plant. It is shown that the presented modular electrolysis systems can follow the current flow without losing significant efficiency. However, for a downstream system that requires a constant hydrogen mass flow, supplementary hydrogen storage is required.

Keywords: Energy Efficiency, Hydrogen, Process Design, Energy Systems, Renewable and Sustainable Energy, Flexibility, Lange-Große-Coefficient

BACKGROUND

Hydrogen has a thermal and material application (purpose) in shaft furnaces. On the one hand, hydrogen is used to reduce the iron ore, and on the other hand for combustion and the associated melting of the iron ore. However, an electrolysis system is needed to provide this hydrogen. The electrolysis system presented here is to be modularly constructed and heterogeneously scaled. The concept and structure of individual modular electrolysis systems have already been explained in the past [2–4]. A heterogeneously scaled electrolysis system is understood to be the numbering-up of different electrolysis technologies in different sizes in one overall electrolysis system. That way technology-specific advantages, like high efficiency or increased energy input flexibility, can be harnessed more efficiently [5]. Due to an increasing amount of renewable energy in the grid, the price of electricity is also fluctuating more throughout the day. In general, it can be said that the electricity price is lowest when the proportion of renewable energies in the electricity mix is high [6]. These temporal fluctuations need to be harnessed by designing flexible control strategies for large-scale electrolysis systems, that can follow them. Using heterogeneous electrolysis systems can provide a bigger operational window and higher flexibility for such fluctuating power inputs while maintaining high efficiency of hydrogen production resulting in lower hydrogen cost.

METHODS & IMPLEMENTATION

Assumptions

An average fictional steelworks with a production capacity of 125,000 kg/h of briquetted sponge iron was set up as a boundary condition [7–9]. To produce the mass flow of briquetted sponge iron, a minimum of 6364 kg/h of H2 are required. This can be calculated from the stoichiometry in the reduction equation in (1).

$$Fe_2O_3 + 3\,H_2 \rightarrow 2\,Fe + 3\,H_2O\ \Delta H_R = 99{,}5\ kjmol^{-1} \qquad (1)$$

This calculated minimum requirement shall define the lower boundary of the demand side. To define the fluctuating energy side, synthetic 'Solar Power Data for Integration Studies' data from the National Renewable Energy Laboratory for the state of New York [10] is used as a initial scenario. The data was created specifically for system integration studies, as in this study. The solar power data consists of 5-minute solar power data with hourly Day-Ahad forecasts and refers to the year 2006. The data generated from the 5-minute data set was developed by NREL using a 'Sub-Hour Irradiance Algorithm' [10]. The first week of January and the first week of July of this 5-minute time-step data were extracted and the data was normalized against the maximum within the sample set to define the operating point inputs between zero load and nominal load of the electrolysis system.

As shown in Table 1 the scaled modular and heterogeneous electrolysis system consists of aggregated blocks of both the electrolysis technologies alkaline electrolysis (AEL) and the proton exchange membrane electrolysis (PEMEL), as these two are the technologies with the highest technology readiness level (TRL). In our design an AEL block consists of eight AEL stack units with an output of 5 MW each that are connected to a lye circulation module. A PEMEL block consists of two PEMEL stack units with an output of 2 MW each that are connected to a DI-water circulation module [3,11]. A DI-water circulation module is a process engineering unit that has been specially developed for the circulation of treated water through the satellite unit. It also takes over the separation of product gases hydrogen and oxygen from the water circuit [3,11]. An efficiency of η_{AEL}= 0.68 was assumed for the AEL and an efficiency of η_{PEMEL}= 0.63 for the PEMEL relative to the lower heating value of hydrogen [11].

Another assumption is that at least one AEL block is always operated to ensure a minimum hydrogen volume flow for the subsequent process. This is since AEL cannot react as quickly to power changes and has a higher efficiency than PEMEL, which makes it more interesting for constant operation. The AEL was assumed to have a load gradient of 30 %/s ramp-up and 10 %/s ramp-down while the load gradients of the PEMEL are 50 %/s in ramp-up and 40.6 %/s in ramp-down. [11]

Optimization problem

The hydrogen mass flow generated can be approximately calculated according to equation (1), where the nominal power of the two electrolysis technologies in hydrogen production are multiplied with their respective system efficiency and divided by the gravimetric calorific value of hydrogen, which is 33.33 kWh kg^{-1} [12].

$$\dot{m}_{max}\,[\frac{kg}{h}] = \frac{A \cdot 8 \cdot 5000[kW] \cdot \eta_{AEL} + B \cdot 2 \cdot 2000[kW] \cdot \eta_{PEM}}{33{,}33\,[\frac{kWh}{kg}]} \qquad (1)$$

The variables 'A' and 'B' presented in Formula (2) and (3) are used to calculate the distribution of the AEL and PEMEL. The variable 'A' represents a selected number of AEL blocks, starting with 0 blocks, scaled up step by step to 10 AEL blocks. The variable 'B' represents the corresponding number of PEMEL blocks, which can be calculated with the maximum hydrogen massflow given, using formula (2):

$$B\,[-] = \frac{\dot{m}_{max}[\frac{kg}{h}] \cdot 33{,}33[\frac{kWh}{kg}] - A \cdot 8 \cdot 5000[kW] \cdot \eta_{AEL}}{2 \cdot 2000[kW] \cdot \eta_{PEM}} \qquad (2)$$

As boundary conditions, the number of respective technology blocks, A and B, cannot be below a set minimum threshold. For these first evaluations, the threshold has been set to 0.

$$A > A_{min}$$
$$B > B_{\min} \qquad (3)$$

Table 1: Configurations of aggregated AEL and PEMEL blocks

Config.	AEL	PEMEL
0	0	109
1	1	98
2	2	87
3	3	76
4	4	66
5	5	55
6	6	44
7	7	33
8	8	22
9	9	11
10	10	0

As this is to be a heterogeneous electrolysis system, both electrolysis technologies must be installed in one electrolysis system. The fifrst scaling configuration is an AEL block in conjunction with 91 PEMEL blocks. Based on this, the AEL blocks are now gradually increased up to eight AEL blocks while simultaneously reducing the number of PEMEL blocks to keep the total H_2 capacity (1 AEL block equals 11 PEMEL blocks). Table 1 shows the eleven possible configurations of AEL and PEMEL blocks.

The overall efficiency of the electrolysis system is calculated from the number of blocks in the system and the individual efficiencies of the electrolysis technologies using equation (4). The values of the individual efficiencies were taken from [11].

$$\eta_{sys}\,[-] = \frac{A \cdot 8 \cdot 5000[kW] \cdot \eta_{AEL} + B \cdot 2 \cdot 2000[kW] \cdot \eta_{PEM}}{A \cdot 8 \cdot 5000[kW] + B \cdot 2 \cdot 2000[kW]} \quad (4)$$

To evaluate the system flexibility the Expected Unserved Flexible Energy (EUFE) value is calculated for the described input scenario of solar power input in 5-minute time-steps [13]. The power input behavior of the electrolyzer blocks is simplified, using the load gradient parameters for a linear load ramp-up and ramp-down from Lange et al. [11]. The EUFE can now be determined from the specified operating point of the scenario and the actual operating point of the electrolysis system, following the requested load changes of the solar power input profile. Often the EUE value is also used for this, which stands for "Expected Unserved Energy", but both describe the same thing [14]. According to equation (5), the power of the scenario is subtracted from the power of the actual operating point at each time step and integrated over the period under consideration.

$$EUFE\,[kWh] = \int abs((P_{scenario}(t) - P_{system}(t))dt \quad (5)$$

One problem with the EUFE value is the comparability of different scenarios and systems. As this is a continuous summation of the differences in output, the EUFE value is heavily dependent on the consideration of the time length of the scenario and the system under consideration. Therefore, the authors of this study aim to modify the EUFE value to consider the flexibility of a system that is more independent of the scenario under consideration and the system performance of the system under consideration. For this purpose, the EUFE value is related to the integrated power input of the scenario. The resulting value represents the share of energy in the scenario that cannot be utilized by the system under consideration. This value is referred to below as the "Lange-Große-Coefficient" (LGC) and is calculated using equation (6):

$$LGC = \frac{EUFE}{\int P_{scenario}(t)dt} \quad (6)$$

The Levelized Cost of Hydrogen (LCOH) was also calculated according to [15].

$$M = \begin{cases} y = f(\eta, LGC, LCOH, \dot{m}_{H_2}) \\ \quad s.t. LGC \leq 5\% \\ \quad s.t. \dot{m}_{H_2} \geq \dot{m}_{max} \end{cases} \quad (7)$$

Equation (7) describes the model of the optimisation problem.

DISCUSSION

The system configurations listed in Table 1 were simulated in MATLAB/Simulink. The results are summarized in

Figure 2. The dots reflect the LGC (see equation (6)) against the system efficiency, the triangles the calculated LCOH against the system efficiency. The LGC increases linearly with the system efficiency, which is due to the increase in AEL in the overall system. In contrast, the LCOH behaves inversely proportional and decreases with the increase of the AEL in the overall system. If the LGC must not rise above a value of 5%, configurations 7-10 would not apply.

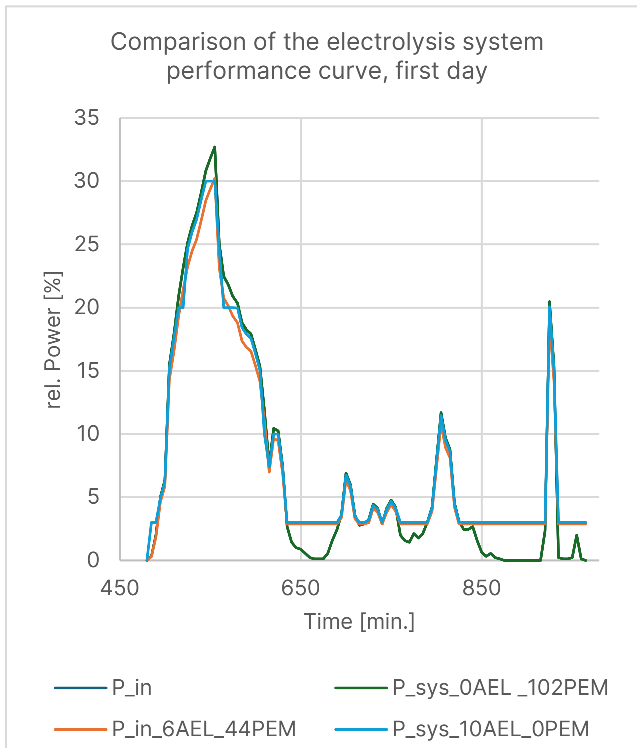

Figure 1: Comparison of the system outputs of the optimum case (Con. 6, orange line) and the two marginal cases (Con. 0, green line and Con. 10, blue line) with the outputs entering the electrolysis system to illustrate the 'start-stop principle' operating strategy [11,16]. Due to the absence of the AEL and the associated base load in Con. 0, smaller partial load ranges below 3% are also utilised.

Configuration 0 with a 100% share of PEMEL represents the first edge case. In contrast to the systems with AEL blocks there is no base load component in this edge case. As a result, every change in the input power is adopted, which means that the LGC is higher than in configuration 1. This shows, that the LGC needs further adjustments become even more independent of the flexibility requests of the input scenario. With the introduction of the base load by the AEL, the LGC decreases, while at the same time increasing the system efficiency. The second edge case is configuration 10 with a 100% AEL share. Here it is the case that when the minimum load of the AEL is reached, only the start-stop principle is used [11].

The two edge cases consisting of 100% PEMEL (configuration 0) and 100% AEL (configuration 10) are included in the analysis of the modular and heterogeneous electrolysis system. These two modular homogeneous scaling cases show anomalies, as can be seen in Figure 2. For the configuration, the increase in LGC is due to the distribution of power within the system. No minimum load was initially defined for the PEMEL, which enables the PEMEL to follow the power and the associated flexibility signals exactly. Flexibility signals are time steps at which the incoming power into the system changes, to which the system in turn must react. As soon as the AEL is added to the system, flexibility signals that are below the minimum load are ignored and are therefore not included in the calculation of the LGC, which is why the LGC drops in the first configuration.

The second edge case in configuration 10 shows a drop in the LGC. This is since anomalies also occur during system start-up, just as during system shutdown. With a start-stop strategy that only allows the system to be operated at 100% power, flexibility signals that are not sufficient to start up an entire AEL block are ignored. This leads to a reduction in the LGC. This lack of capacity was compensated for by the PEMEL in the previous configuration. One solution could be to shut down an AEL block to start a new one. This must be done on the condition that it is known that the incoming power will continue to increase. One solution could be to shut down an AEL block in order to start a new one. This must be done on the condition that it is known that the incoming power will continue to increase. The shutdown behavior of the system can also be further optimized. Here, several AEL units could initially be run in a partial load range instead of taking entire units out of operation. This would have an additional effect on the efficiency of the system, as the AEL systems are more efficient in the partial load range. Optimisation can still take place for both edge cases, as the same operating strategy was selected for the modular homogeneous systems as for the modular heterogeneous systems to establish comparability.

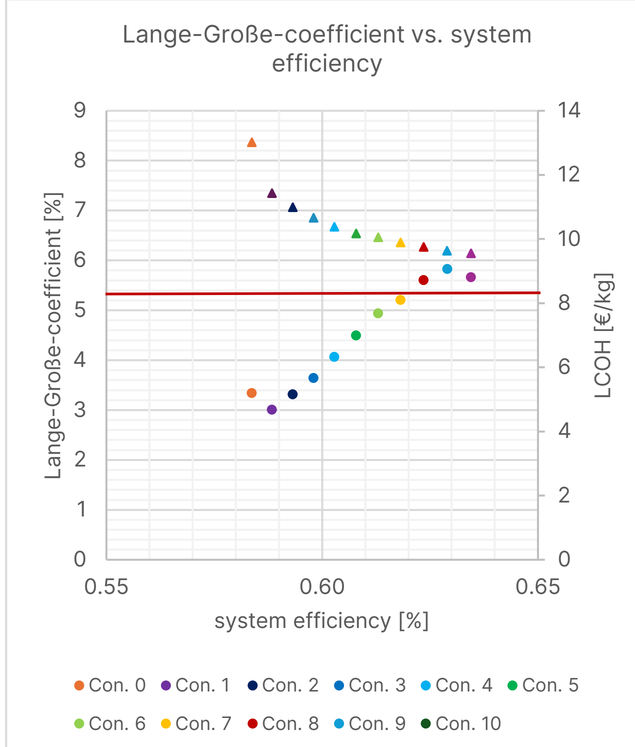

Figure 2: Lange-Große-Coefficient (LGC) and Levelised Cost of Hydrogen (LCOH) vs. system efficiency. All modular heterogeneous system configurations from Table 1 (Con. 1-9) are shown, including the two edge cases for modular homogeneous system configurations (Con. 0 and Con 10). The LGC is represented by a dot in the diagram, the LCOH by a triangle, and each configuration has its own colour. Dabei ist ein Abfallen der LCOH mit steigender A drop in the LCOH can be recognised with increasing system efficiency, which is the same for Con. 8 reaches a minimum. The LGC increases linearly with increasing system efficiency, if the two marginal cases are disregarded.

The weighted optimum is the sum of the system efficiency, the LGC and the LCOH. For this purpose, the LCOH is normalised and related to the lowest value. The same is done for the LGC. For both values, a low value is better than a high one. The system efficiency is also normalized to the value. The rule here is that a high system efficiency is better. The sum of these three normalized values can now only be between 0 and 3. As shown in the Figure 3 weighted optimum drops further with each configuration. With the previously established boundary condition that the LGC should not be above 5%, configuration 6 turns out to be the optimal distribution between AEL and PEMEL.

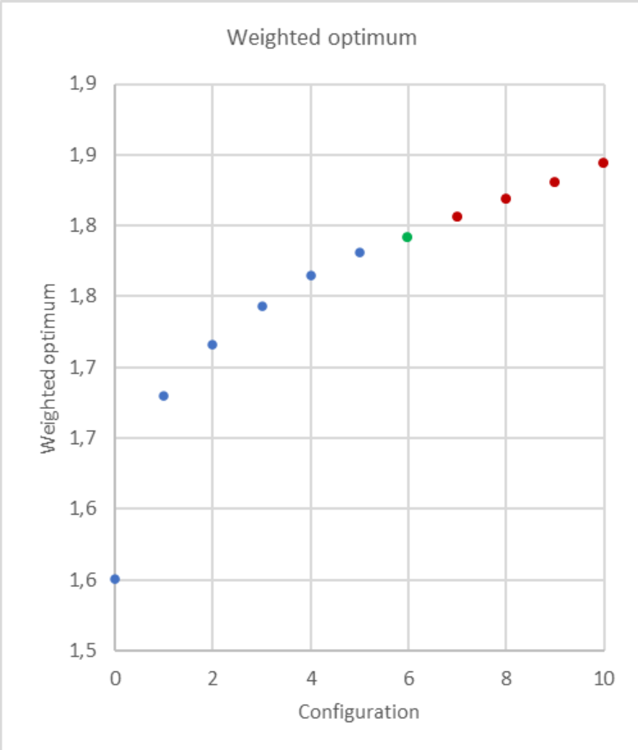

Figure 3 The weighted optimum for all configurations. Configuration 6 is marked in green, all configurations outside the 5% limit of the LGC are marked with red dots.

CONCLUSION

As has been shown, a fluctuating current curve can be followed with the modular heterogeneous electrolysis systems shown. This results in an optimum within the distribution of electrolysis technologies. An optimally composed electrolysis system consisting of 58% AEL and 42% PEMEL was determined for the scenario shown for an average fictional steelworks. With this composition, high efficiency at low LCOH can be guaranteed in a system that is able to respond to flexibility signals with an LGC of less than 5%. This system composition is therefore to be favored in operation. While the LCOH between configuration 6 and 10 fluctuate by 0.51 €/kg H2, the LGC between these two configurations fluctuates by 0,75%. To put this into perspective, the LCOH decreases between configurations 1 and 6 by 2.98 €/kg. Although an electrolysis system consisting purely of AEL has lower operating costs of 0.51 €/kg, it cannot react as quickly to power fluctuations. This flexibility advantage can be useful in the future, especially with flexible electricity tariffs.

OUTLOOK

As shown in the previous section, the LGC must be made even more scenario-independent. No flexibility signals below the minimum load should be ignored. If flexibility signals cannot be served, this must be included in the LGC to ensure full comparability with the marginal cases.

Furthermore, the load distribution within an electrolysis system must be further adapted. As has been shown, the LGC can be reduced even further with a further customized operating strategy. A comparison of different operating strategies in a modular heterogeneous plant design with different electrolysis technologies must be investigated further; the foundations for this have already been laid in [11,16].

Another point is the simulative integration of high temperature electrolysis (HTEL) into a system with AEL and PEM. Here it may be possible to further increase the base load efficiency by extracting heat and the associated vaporization of water for the HTEL.

Furthermore, the relationship between a fluctuating current input and a subsequent process such as direct iron reduction after electrolysis, which requires a constant hydrogen mass flow, is still unclear. At this point, energy storage is required, either on the electricity or the hydrogen side of the process. A suitable method needs to be developed to define the right ratio between electricity and hydrogen storage.

ACKNOWLEDGEMENTS

We would like to thank the German Federal Ministry of Education and Research and the project management organization Jülich for their financial support within the framework of the eModule research project (FKZ 03HY116A) of the H2Giga lead platform. Furthermore, the P2O-Lab Learning Factory of the TUD Dresden University of Technology is thanked for its support.

REFERENCES

1. Wietschel M, Zheng L, Arens M, Helbing C, Ranzmeyer O, Schaadt A, et al. Metastudie Wasserstoff – Auswertung von Energiesystemstudien. Studie im Auftrag des Nationalen Wasserstoffrats. Karlsruhe, Freiberg, Cottbus: 2021.
2. Bittorf L, Beisswenger L, Erdmann D, Lorenz J, Klose A, Lange H, et al. Upcoming domains for the MTP and an evaluation of its usability for electrolysis. 2022 IEEE 27th international conference on emerging technologies and factory automation (ETFA), 2022, p. 1–4. https://doi.org/10.1109/ETFA52439.2022.9921280
3. Lange H, Klose A, Beisswenger L, Erdmann D, Urbas L. Modularization approach for large-scale electrolysis systems: a review. Sustainable Energy Fuels 2024:10.1039.D3SE01588B. https://doi.org/10.1039/D3SE01588B

4. Lange H, Schirmer C, Mock M, Viedt I, Klose A, Urbas L. Operation Strategies for Modular Large-Scale Alkaline Electrolysis Systems. 2024 IEEE 22nd International Conference on Industrial Informatics (INDIN), Beijing, China: IEEE; 2024, p. 1–7. https://doi.org/10.1109/INDIN58382.2024.10774361
5. Mock M, Viedt I, Lange H, Urbas L. Heterogenous electrolysis plants as enabler of efficient and flexible Power-to-X value chains. Computer Aided Chemical Engineering, vol. 53, Elsevier; 2024, p. 1885–90. https://doi.org/10.1016/B978-0-443-28824-1.50315-X
6. ISE F. Day-ahead auktion vs. Solar + wind onshore + wind offshore in deutschland, 2022. Energy-Charts 2023.
7. Albrecht U, Ball M, Bünger U, Kutz C, Michalski J. Metastudie zu den technischen, technologischen und wirtschaftlichen Parametern für die Umstellung der deutschen Stahlindustrie auf eine emissionsarme Stahlproduktion auf Basis von grünem Wasserstoff 2022.
8. Hölling M, Weng M, Gellert S. Bewertung der Herstellung von Eisenschwamm unter Verwendung von Wasserstoff (Evaluation of the production of sponge iron using hydrogen). Eisen & Stahl 2017;6:47–56.
9. Nuber D, Eichberger H, Rollinger B. Circored fine ore direct reduction. MILLENNIUM STEEL 2006:37–40.
10. National Renewable Energy Laboratory. Solar Power Data for Integration Studies 2024. https://www.nrel.gov/grid/solar-power-data.html (accessed November 14, 2024).
11. Lange H, Klose A, Lippmann W, Urbas L. Technical evaluation of the flexibility of water electrolysis systems to increase energy flexibility: A review. International Journal of Hydrogen Energy 2023;48:15771–83. https://doi.org/10.1016/j.ijhydene.2023.01.044.
12. VDI e. V., editor. VDI-Wärmeatlas. Berlin, Heidelberg: Springer Berlin Heidelberg; 2013. https://doi.org/10.1007/978-3-642-19981-3
13. Gusain D, Cvetkovic M, Palensky P. Quantification of operational flexibility from a portfolio of flexible energy resources. International Journal of Electrical Power & Energy Systems 2022;141:107466. https://doi.org/10.1016/j.ijepes.2021.107466
14. Fazio J, Hua D. Three probabilistic metrics for adequacy assessment of the Pacific Northwest power system. Electric Power Systems Research 2019;174:105858. https://doi.org/10.1016/j.epsr.2019.04.036
15. European Hydrogen Observatory. Levelised Cost of Hydrogen (LCOH) Calculator 2024.
16. Lorenz J, Klose A, Lange H, Kock T, Urbas L. Flexible Process Control for Scalable Electrolysis Systems. III. International Conference on Electrical, Computer and Energy Technologies (ICECET 2023), Cape Town-South Africa: IEEE; 2023. https://doi.org/10.1109/ICECET58911.2023.10389401.